Chinese Journal of Natural Medicines

Exploring the mechanism of Xiaoaiping Injection inhibiting autophagy in prostate cancer based on proteomics

Qiuping Zhang, Qiuju Huang, Zhiping Cheng, Wei Xue, Shoushi Liu, Yunnuo Liao, Xiaolan Li, Xin Chen, Yaoyao Han, Dan Zhu, Zhiheng Su, Xin Yang, Zhuo Luo, Hongwei Guo

Citation: Qiuping Zhang, Qiuju Huang, Zhiping Cheng, Wei Xue, Shoushi Liu, Yunnuo Liao, Xiaolan Li, Xin Chen, Yaoyao Han, Dan Zhu, Zhiheng Su, Xin Yang, Zhuo Luo, Hongwei Guo, Exploring the mechanism of Xiaoaiping Injection inhibiting autophagy in prostate cancer based on proteomics, Chinese Journal of Natural Medicines, 2025, 23(1), 64−76. doi: 10.1016/S1875−5364(25)60804−1.

View online: https://doi.org/10.1016/S1875−5364(25)60804−1

Chinese Journal of Natural Medicines 23 (2025) 64-76

Contents lists available at ScienceDirect

Chinese Journal of Natural Medicines

journal homepage: www.cjnmcpu.com/

Original article

Exploring the mechanism of Xiaoaiping Injection inhibiting autophagy in prostate cancer based on proteomics

Qiuping Zhang[a,b,c,Δ], Qiuju Huang[b,Δ], Zhiping Cheng[b,Δ], Wei Xue[b,c], Shoushi Liu[b,c], Yunnuo Liao[b,c], Xiaolan Li[b,c], Xin Chen[b,c], Yaoyao Han[b,c], Dan Zhu[b], Zhiheng Su[b], Xin Yang[c,*], Zhuo Luo[b,*], Hongwei Guo[b,c,*]

[a] *Department of Traditional Chinese Medicine, the First Affiliated Hospital of Guangxi Medical University, Nanning 530021, China*
[b] *Guangxi Key Laboratory of Bioactive Molecules Research and Evaluation & College of Pharmacy, Guangxi Medical University, Nanning 530021, China*
[c] *Key Laboratory of Longevity and Aging-related Diseases of Chinese Ministry of Education & Center for Translational Medicine, Guangxi Medical University, Nanning 530021, China*

ARTICLE INFO

Article history:
Received 11 January 2024
Revised 7 April 2024
Accepted 28 May 2024
Available online 20 January 2025

Keywords:
Xiaoaiping Injection
Autophagy
Apoptosis
Forkhead box O3a
Prostate cancer

ABSTRACT

Xiaoaiping (XAP) Injection demonstrates the anti-prostate cancer (PCa) effects, yet the underlying mechanism remains unclear. This study aims to investigate the impact of XAP on PCa and elucidate its mechanism of action. PCa cell proliferation was evaluated using a cell counting kit-8 (CCK-8) assay. Cell apoptosis was assessed through Hoechst staining and Western blotting assays. Proteomics technology was employed to identify key molecules and significant signaling pathways modulated by XAP in PCa cells. To further validate potential key genes and important pathways, a series of assays were conducted, including acridine orange (AO) staining, transmission electron microscopy, and immunofluorescence assays. The molecular mechanism of XAP against PCa *in vivo* was examined using a PC3 xenograft mouse model. Results demonstrated that XAP significantly inhibited cell proliferation in multiple PCa cell lines. In C4-2 and prostate cancer cell line-3 (PC3) cells, XAP induced cellular apoptosis, evidenced by reduced B-cell lymphoma 2 (Bcl-2) levels and elevated Bcl-2-associated X (Bax) levels. Proteomic, immunofluorescence, and quantitative reverse transcription-polymerase chain reaction (qRT-PCR) investigations revealed a strong correlation between forkhead box O3a (FoxO3a) autophagic degradation and the anti-PCa action of XAP. XAP hindered autophagy by reducing the expression levels of autophagy-related protein 5 (Atg5)/autophagy-related protein 12 (Atg12) and enhancing FoxO3a expression and nuclear translocation. Furthermore, XAP exhibited potent anti-PCa action in PC3 xenograft mice and triggered FoxO3a nuclear translocation in tumor tissue. These findings suggest that XAP induces PCa apoptosis *via* inhibition of FoxO3a autophagic degradation, potentially offering a novel perspective on XAP injection as an effective anticancer therapy for PCa.

1. Introduction

Prostate cancer (PCa), one of the most prevalent malignancies in the male urogenital system, is a primary contributor to cancer-related deaths in males [1]. The global burden of disease (GBD) survey reports that the overall incidence and mortality of PCa in China are gradually increasing, with a trend towards affecting younger populations [2]. The treatment of PCa currently faces significant challenges. Patients with PCa often do not exhibit overt symptoms until the disease has advanced. Furthermore, PCa patients are prone to developing chemoresistance, which can lead to fatal castration-resistant PCa, complicating treatment efforts. Consequently, the development of safe and effective alternative medications for PCa treatment is of critical importance.

Traditional Chinese medicine (TCM) has demonstrated significant efficacy in cancer treatment, offering diverse targets, reduced adverse effects, and the ability to overcome drug resistance [3, 4]. Recent studies highlight the unique advantages of TCM prescriptions in treating PCa, including tumor mass reduction and prolonged survival rates [5, 6]. Xiaoaiping (XAP) Injection, a TCM formulation derived from *Marsdenia tenacissima* (Roxb.), originates from a plant predominantly cultivated in Yunnan, Guangxi, and Guizhou Provinces. This plant is known for its heat-eliminating, diuretic, expectorant, and fire-purging properties. Traditionally, the dried cane of *Marsdenia tenacissima* was employed to treat various conditions, including sore carbuncles, rheumatic swelling discomfort, breast milk blockage, and cough [7]. In recent clinical applications across China, XAP Injection (also known as Tong-Guan-Teng Injection) has exhibited multiple therapeutic benefits for advanced non-small cell cancer (NSCLC) and cancers of the esophagus, liver, stomach, and breasts [8-11].

* Corresponding author.
E-mail addresses: xiny1301@Hotmail.com (X. Yang); luozhuo@gxmu.edu.cn (Z. Luo); hongweiguo@gxmu.edu.cn (H. Guo)
Δ These authors contributed equally to this work.

https://doi.org/10.1016/S1875-5364(25)60804-1

Numerous investigations have explored the fundamental mechanisms by which XAP combats cancer [12-14]. The anticancer effects of XAP involve several processes, including the induction of cellular apoptosis [15], modulation of the tumor microenvironment (TME) [16], cell cycle arrest [17], and influence on angiogenesis [18]. However, recent research focusing specifically on XAP's effects on PCa remains limited.

Wang et al. [19] conducted the first clinical study of XAP treatment for PCa, involving 100 patients. The results indicated that XAP could be a viable anti-PCa treatment in clinical practice. Our most recent research revealed that XAP suppresses PCa cell proliferation *via* the ErbB2-GSK3β-HIF1α signaling axis [20]. However, the precise mechanisms of XAP treatment's pharmacological activity that induce PCa cell death remain unknown and require further investigation. Consequently, this study primarily focused on elucidating the mechanisms by which XAP causes PCa cell death. The findings demonstrate that XAP inhibits FoxO3a's autophagic degradation, which enhances FoxO3a nuclear translocation and ultimately induces PCa cell apoptosis. FoxO3a is recognized as a tumor suppressor gene [21] and is involved in multiple cellular physiological activities, including apoptosis [22], autophagy [23], cell cycle progression [23], and drug resistance [24]. Additionally, FoxO3a participates in a homeostatic feedback surveillance loop that maintains autophagy homeostasis, ensuring that cells failing to re-establish proper autophagy levels are more likely to undergo apoptosis when autophagy is inhibited [25, 26]. Thus, this study demonstrates that XAP-induced apoptosis depends on FoxO3a accumulation, providing novel insights into XAP as a potential clinical treatment for PCa.

2. Materials and methods

2.1. Chemicals

XAP Injection, marketed under the trade name Tong-Guan-Teng Injection, was obtained from Nanjing Sanhome Pharmaceutical Co., Ltd. (Nanjing, China). Paclitaxel (PTX, Cat. 33069-62-4) was procured from Med Chem Express (Monmouth Junction, NJ, USA). Sigma (Milwaukee, WI, USA) supplied Rapamycin (Rapa, Cat. V900-930-1MG).

2.2. Characterization of XAP's components

XAP (5 mL), after desiccation with nitrogen, was reconstituted in methanol (1 mL). Following established protocols, the chemical composition of XAP was determined using high-performance liquid chromatography-charge aided detection-quadrupole time-of-flight mass spectrometry/mass spectrometry (HPLC-CAD-QTOF-MS/MS) after filtration through a microporous membrane (0.22 μm) [20].

2.3. Cell culture

The Research Center of Translational Medicine (Guangxi Medical University, China) supplied PCa cell lines LNCap, DU145, C4-2, and PC3. These PCa cell lines were cultured in RMPI-1640 medium (Cat. 350-006-CL, WISENT, Canada) supplemented with 10% fetal bovine serum (FBS, Cat. 10099141C, Gibco, USA) and 1% penicillin-streptomycin (Cat. 450-201-EL, WISENT, Canada). The cells were maintained in a cell incubator at 37 °C with 5% CO_2.

2.4. Assessment of cell proliferation

C4-2 and PC3 cells were suspended in RPMI-1640 media and seeded in 96-well plates (Costar) at a density of 3 × 10^3 cells/well. The cells were then treated with varying concentrations of XAP (0, 10, 20, 40, 80, 160, and 320 mg·mL^{-1}). After 24 and 48 h of incubation, cell counting kit-8 (CCK-8) reagent (AR1199, PerkinElmer, USA) was added to the cells and incubated at 37 °C for 30 min. Subsequently, the absorbance (optical density, OD) was measured at 450 nm using a microplate reader [Model Multiskan Gene Ontology (GO), Thermo Fisher, USA]. Cell viability was calculated using the following equation: cell viability = $[(OD_{sample} - OD_{blank})/(OD_{control} - OD_{blank})] \times 100\%$.

2.5. Analysis of proteomics comparison

Monitor Helix BioTech Co., Ltd. (Shanghai, China) conducted a comparative proteome analysis. PC3 cells were treated with XAP Injections (0 and 60 mg·mL^{-1}) for 24 h. Total protein was extracted from the samples using a lysis buffer (Cat. 89900, Thermo Fisher, USA) and quantified using the Bradford protein assay kit (Cat. P0006, Beyotime) according to the manufacturer's instructions. Sequencing grade modified trypsin was used to digest each sample's protein pool at ratios of 50∶1 for 4 h and 100∶1 overnight at 37 °C. Following trypsin digestion, peptides were desalinated and vacuum-dried on Waters hydrophilic-lipophilic balanced columns (HLB) columns. The dried and labeled peptides were reconstituted in HPLC solution A (2% ACN, pH 10) and fractionated using Waters Bridge Peptide BEH C_{18} by high pH reverse-phase HPLC (130 Å, 3.5 μm, 4.6 mm × 250 mm), followed by liquid chromatography-tandem mass spectrometry (LC-MS/MS) analysis. The MS/MS data were searched against the Homo Sapiens database, comprising a reviewed Swissprot database containing 20 404 protein sequences (Taxon identifier: 9606). Differentially expressed proteins (DEPs) were defined as those with fold changes between the two comparison groups of > 1.2 or < 0.83 and a significant *t*-test *P*-value < 0.05. GO function and Kyoto Encyclopedia of Genes and Genomes (KEGG) pathway enrichment analyses were subsequently performed on the identified DEPs.

2.6. Transmission electron microscopy (TEM)

PC3 cells were collected 24 h after XAP Injections (0 and 60 mg·mL^{-1}) and fixed overnight in 2.5% glutaraldehyde. Following treatment with a fixative containing 2% osmium tetroxide, the samples were dehydrated using gradient alcohol. The alcohol in the sample was then replaced with anhydrous epoxy-propane or acetone, repeating this process three times before adding epoxy resin. A catalyst-epoxy resin mixture (3∶4) was added to the embedding mold, and the sample was oriented appropriately before initiating polymerization in an oven. For TEM analysis, the samples were cut into ultra-thin sections and mounted on copper grids.

2.7. Hoechst staining

PCa cells were seeded in 12-well plates and incubated overnight. Following 24 h of exposure to XAP (0, 30, and 60 mg·mL^{-1}), the cells were fixed with 4% formaldehyde for 30 min. Subsequently, the cells were rinsed with phosphate-buffered saline (PBS) and stained with Hoechst 33258 (BL804A, Biosharp, China) for 10 min. Cells were observed using a fluorescent microscope at an excitation wavelength of 350 nm and an emission wavelength of 461 nm. The fluorescence density of nuclei was analyzed using ImageJ software, with a minimum of 200 cell counts for each concentration.

2.8. Acridine orange (AO) staining

During autophagy, cytoplasmic proteins or organelles encapsulated by autophagosomes fuse with lysosomes to form auto-

lysosomes, leading to the degradation of the encapsulated contents. To visualize acidic intracellular compartments, supravital AO staining was employed. Cells were exposed to XAP (0 and 60 $mg·mL^{-1}$) for 24 h, then rinsed in PBS, and labeled with 5 $μg·mL^{-1}$ AO (Cat. 10127-02-3, Macklin, China) at 37 °C for 10 min. Subsequently, the cells were examined under a fluorescent microscope (Model IX71, Olympus, USA).

2.9. Western blotting assay

A 24-h XAP treatment was administered to cells after seeding them into a 10-cm petri dish. As described in a previous publication [27], a bicinchoninic acid (BCA) protein assay kit was employed to quantify the total proteins extracted *via* radioimmunoprecipitation assay (RIPA) lysis (Cat. 23227, Thermo Fisher, USA). Subsequently, equal quantities of proteins per sample were electrophoresed using 8%–15% SDS-PAGE and then transferred onto a polyvinylidene difluoride (PVDF) membrane (IPVH00010-26, Solarbio). After blocking, the membranes were incubated with primary antibodies at 4 °C overnight. The protein bands were visualized following exposure to the relevant immunofluorescence secondary antibodies. ImageJ software was utilized to derive and normalize the protein expression levels to the control.

2.10. Immunofluorescence

PCa cells were seeded onto 12-well plates and treated with XAP (0, 30, and 60 $mg·mL^{-1}$) for 24 h. The cells were then fixed with 4% paraformaldehyde (PFA), permeabilized with 0.5% Triton X-100 (P0096, Beyotime, Shanghai, China), blocked for 30 min with 5% FBS, and incubated overnight with an anti-FoxO3a antibody (1∶200, Cell Signaling, USA). After rinsing with PBS, the cells were incubated for 1 h with a FITC-conjugated secondary antibody. Nuclei were labeled with DAPI (Cat. 010020, SouthernBiotech, USA), and the cells were examined using a fluorescent microscope. The percentage of cells exhibiting FoxO3a-positive expression in the nucleus was evaluated for each group, and three independent experiments were conducted to obtain statistical data.

2.11. Quantitative reverse transcription-polymerase chain reaction (qRT-PCR) assay

Total RNA was extracted from PC3 cells using TRIzol reagent (Cat. 15596026, Invitrogen, USA) and subsequently synthesized into cDNA using the transcriptor first strand cDNA synthesis kit (Cat. R323-01, Vazyme, USA). Relative gene expression profiles were measured using SYBR Green Master Mix and an Applied Biosystems 7300 Real-Time PCR System (Applied Biosystems). GAPDH served as the internal reference. The specific details of the primers are listed in Table S1.

2.12. PC3 xenograft mouse model and treatments

Male BALB/c-nude mice, aged 6 weeks, were obtained from Hunan SJA Laboratory Animal Co., Ltd. (Hunan, China) and maintained in the specific-pathogen-free (SPF)-grade Animal Laboratory of Guangxi Medical University (Registration No. 202204003; April 9, 2022–May 13, 2022). PC3 cells, resuspended in a 0.2% Matrigel∶PBS solution (*W/W*, 1∶1), were implanted subcutaneously into the right flank of mice ($1.8 × 10^6$ cells/mouse) while in an ice bath. Once tumor volumes exceeded 50 mm^3, mice were randomly assigned to the following groups: positive control group (PTX, 20 $mg·kg^{-1}$), high-dose treatment group (XAP, 26 $g·kg^{-1}$), low-dose treatment group (XAP, 13 $g·kg^{-1}$), and control group (0.9% saline). Mice received intraperitoneal injections of PTX once per week or daily administrations of 0.9% saline or XAP. Tumor volume and body weight were recorded every 3 days. After 15 consecutive days of treatment, the mice were euthanized in accordance with Institutional Animal Care and Use Committee (IACUC) guidelines. Tumors and organs were removed, and their weights were measured.

2.13. Hematoxylin and eosin (H&E) staining

After obtaining the organ samples (kidney, lung, spleen, liver, and heart), H&E staining was conducted as outlined before [28]. The sections were stained with hematoxylin for 30 s, followed by exposure to 0.5% eosin for 10 s. A fluorescent microscope (Cat. 010020, SouthernBiotech, USA) was utilized to visualize the sections. The cellular apoptosis ratio was determined by randomly selecting six fields of view (200 ×) per section.

2.14. Terminal deoxynucleotidyl transferase (TdT)-mediated dUTP nick-end labeling (TUNEL) staining

The TUNEL assay was performed using an apoptosis detection kit (Cat. G1502; Servicebio), following previously described protocols [29], to identify apoptotic cells. Examination of the sections was conducted using a fluorescent microscope (Cat. 010020, SouthernBiotech, USA).

2.15. Immunohistochemistry (IHC)

Initially, tumor samples were fixed using 4% PFA, and IHC staining was performed according to previously established protocols [30] . Briefly, the sections were incubated overnight at 4 °C with an anti-FoxO3a antibody (CST2496, 1∶200), followed by a 50-min incubation at room temperature (RT) with horseradish peroxidase (HRP)-conjugated goat anti-rabbit IgG polymer. DAB color development was conducted at RT under microscopic observation with controlled reaction time. For each section, six fields of view at 200 × magnification were randomly selected to quantify positive cells and calculate the average.

2.16. Statistical analysis

Data were presented as the mean ± standard deviation, and all experiments conducted at least three times. Statistical analysis was performed using SPSS version 20. Variations were assessed through one-way analysis of variance (ANOVA), followed by least significant difference (LSD) or Dunnett's T3 tests. A significance threshold was established at $P < 0.05$.

3. Results

3.1. Analysis of XAP's chemical composition

HPLC-CAD-QTOF-MS/MS was employed to analyze the chemical composition of XAP. As shown in Fig. S1, analysis of *m/z* values revealed a total of 21 components in XAP, consistent with our previously published findings [20]. The MS and MS/MS spectra of the 21 XAP compounds are presented in Fig. S1, while Table S2 provides detailed information for each component.

3.2. XAP inhibits PCa cell proliferation in vitro by triggering the apoptotic process

The antiproliferative effect of XAP on PCa cells was evaluated using the CCK-8 assay. Fig. 1A illustrates that XAP significantly reduced the viability of LNCap, C4-2, DU145, and PC3 cells. This reduction was evidenced by the half maximal inhibitory concentration (IC_{50}) values of 149.6 ± 6.83, 177.5 ± 7.61, 177.2 ±

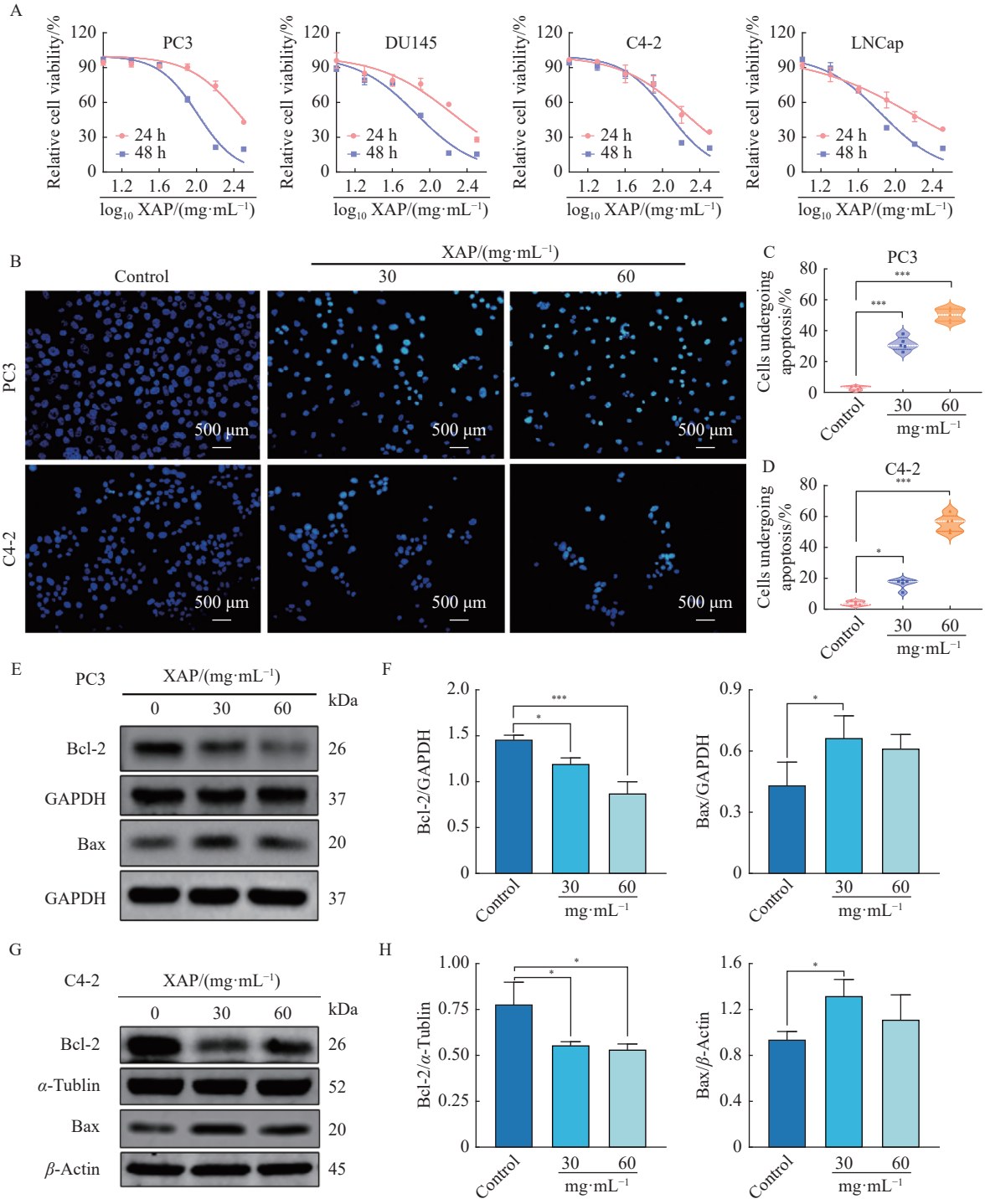

Fig. 1 XAP inhibits PCa cell proliferation *in vitro* by inducing apoptosis. (A) LNCap, C4-2, DU145, and PC3 cells were treated with various concentrations of XAP (0–320 mg·mL^{-1}) for 24 and 48 h, and cell viability was assessed using the CCK8 assay. PC3 and C4-2 cells were treated with XAP at 0, 30, and 60 mg·mL^{-1} for 24 h. (B–D) Hoechst staining was performed to evaluate apoptosis in PCa cells. (E–H) Protein levels of Bax and Bcl-2 in PC3 and C4-2 cells were analyzed by Western blotting. Data are presented as mean ± SD (n = 3). $^{*}P < 0.05$, and $^{***}P < 0.001$ *vs* control.

6.71, and 283 ± 4.16 mg·mL^{-1} after 24 h treatment, and 70.61 ± 4.88, 115.8 ± 7.79, 71.87 ± 3.91, and 102.1 ± 2.36 mg·mL^{-1} after 48 h treatment, respectively. These results indicate that XAP significantly and dose-dependently inhibits PCa cell proliferation. To further investigate the mechanisms underlying the anticancer effects of XAP on PCa cells, C4-2 and PC3 cells were selected for subsequent experiments.

Prior studies have shown that XAP induces apoptosis in various cancer cells, including those from liver, gastric, and colorectal cancers [31-33]. Consistent with our previous findings [34], the apoptotic process in PCa cells significantly increased following XAP treatment. After XAP administration, characteristic morphological changes associated with cell death were observed, including nuclear fragmentation and chromatin condensation (Fig. 1B). Moreover, a dose-dependent increase in the apoptotic percentages of PC3 cells was recorded after XAP treatment, rising from 2.75% ± 0.72% to 31.43% ± 5.96% (30 mg·mL^{-1} XAP) and 48.44% ± 4.05% (60 mg·mL^{-1} XAP) (Fig. 1C). Similarly, C4-2 cells exhibited an increase in their apoptotic percentage from 4.57% ± 1.72% to 15.64% ± 4.21% (30 mg·mL^{-1} XAP) and 56.63% ± 6.97% (60 mg·mL^{-1} XAP) (Fig. 1D). Additionally, Western blotting analysis revealed that XAP administration significantly reduced B-

cell lymphoma 2 (Bcl-2) protein levels while elevating Bcl-2-associated X (Bax) protein levels (Fig. 1E–1H).

3.3. The anti-PCa effect of XAP is associated with the autophagy-related pathway

To comprehensively examine how XAP induces apoptosis in PCa cells, we conducted a comparative proteomics study, identifying 4982 proteins. Following XAP treatment, 59 DEPs were detected, comprising 20 downregulated and 39 upregulated proteins (Fig. 2A). The most enriched DEPs in XAP's anticancer effect included Atg12, PARP1 binding protein (PARPBP), ataxia telangiectasia mutated (ATM), and CUB and Sushi multiple domains 3 (CSMD3). Among these, Atg12, a crucial autophagy molecule, regulates autophagosome formation through Atg12-Atg5 and LC3-II (Atg8-II) complexes [35]. PARPBP and ATM are involved in cell cycle checkpoint, DNA repair, and apoptosis [36-38]. CSMD3, an oncogene, may serve as a biomarker for immunotherapy selection and regulate autophagy [39]. We performed GO function and KEGG pathway enrichment analyses on the 59 identified DEPs.

The growth and homeostasis of cancer cells were associated with aggrephagy, which ranked fourth in the GO enrichment analysis (Fig. 2B). Furthermore, the vacuolar component (Fig. 2C) emerged as the most highly enriched cellular component and is primarily linked to chlamydia infection, selenium, apoptosis, and autophagy [40-42], indicating that autophagy could be one of XAP's key anticancer mechanisms. Moreover, the KEGG pathway enrichment analysis revealed that XAP-induced PCa suppression was closely related to the FOXO signaling pathway (Fig. 2D). FOXO transcription factors are considered tumor suppressors in malignancies due to their ability to induce cell cycle arrest and apoptosis [43]. The FOXO pathway has been reported to play a crucial role in regulating apoptosis and autophagy [44, 45]. Additionally, XAP significantly reduced the expression of Atg12, which is es-

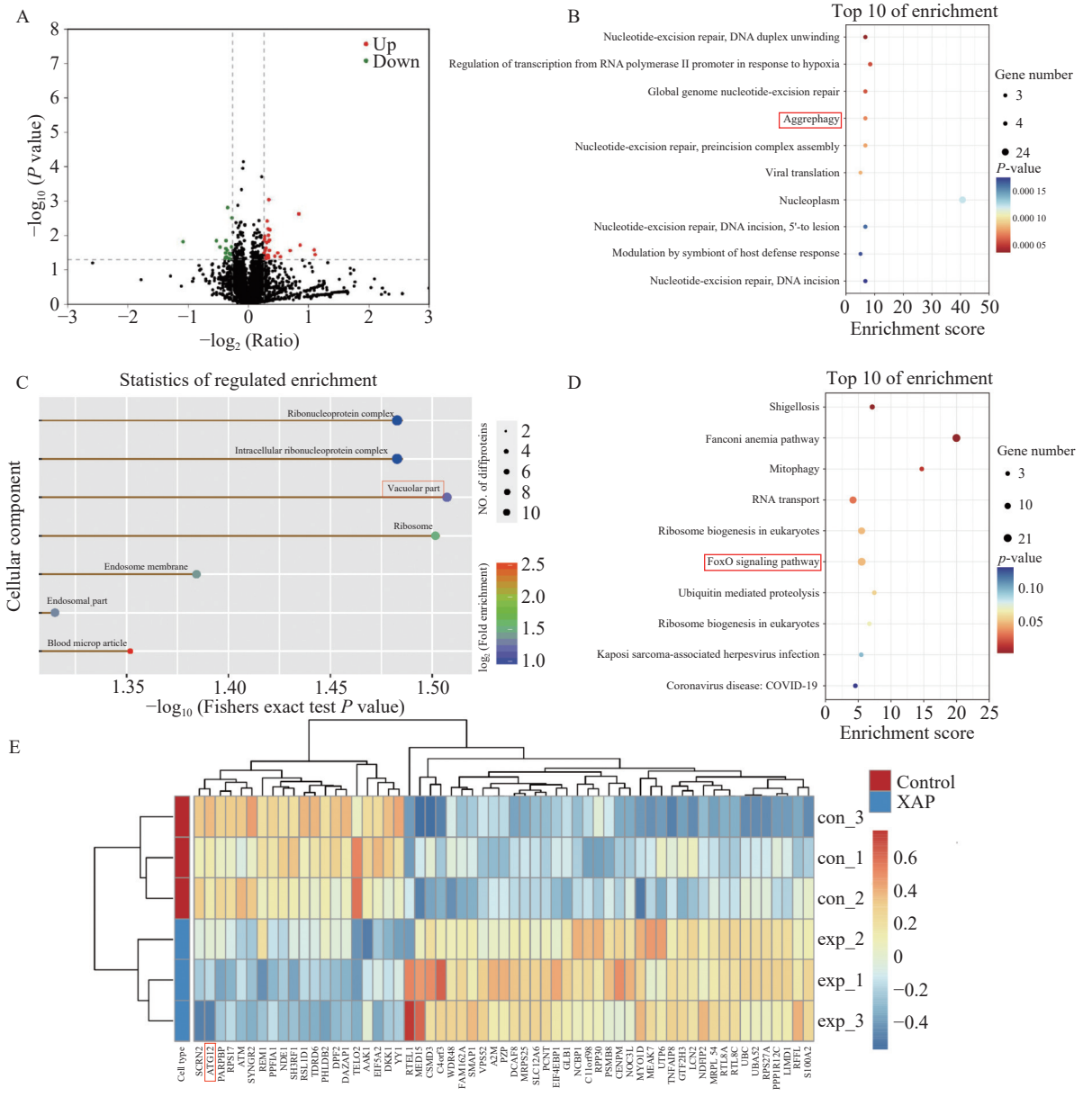

Fig. 2 XAP's anti-PCa effect may be mediated through an autophagy-related mechanism. PC3 cells were harvested for comparative proteomics analysis after 24 h exposure to XAP (0 and 60 mg·mL^{-1}). (A) DEP expression is presented as a volcano plot. A total of 59 DEPs, including 39 upregulated (red points) and 20 downregulated (green points) proteins, were identified using threshold values of FC ≥ 1.2 or ≤ 0.83 and $P < 0.05$. (B) Top ten terms for GO functional enrichment (biological processes, molecular functions, and cellular components). Aggrephagy (noted in red box) ranked fourth. (C) Top ten cellular components. The highest-ranking component was the vacuolar component (highlighted in red box). (D) The FOXO signaling pathway was among the top 10 KEGG pathways (shown by a red box). (E) DEPs are presented as a heatmap. Atg12 was significantly downregulated in PC3 cells, as seen in the red box, indicating potential autophagy inhibition in PC3 cells.

sential for the initiation of autophagy and the formation of autophagy vesicles [46] (Fig. 2E), suggesting that XAP may inhibit autophagy in PCa cells.

3.4. XAP substantially suppresses autophagy in PCa cells

TEM was employed to examine cellular autophagic vesicles to determine if XAP inhibits autophagy in PCa cells. Compared with control group cells, which exhibited monolayer membrane-structured lysosomes and numerous autophagosomes with vacuolar bilayer characteristics, cells in the XAP group demonstrated nuclear fragmentation, decreased cell size, and cellular membrane shrinkage, indicating apoptotic processes (Fig. 3A). AO staining, which changes color from green to red within acidic compartments such as lysosomes and autolysosomes, is frequently utilized as a marker for acidic vesicular organelles [47]. XAP administration reduced red fluorescence in PC3 cells compared with the control group, indicating that XAP treatment significantly de-

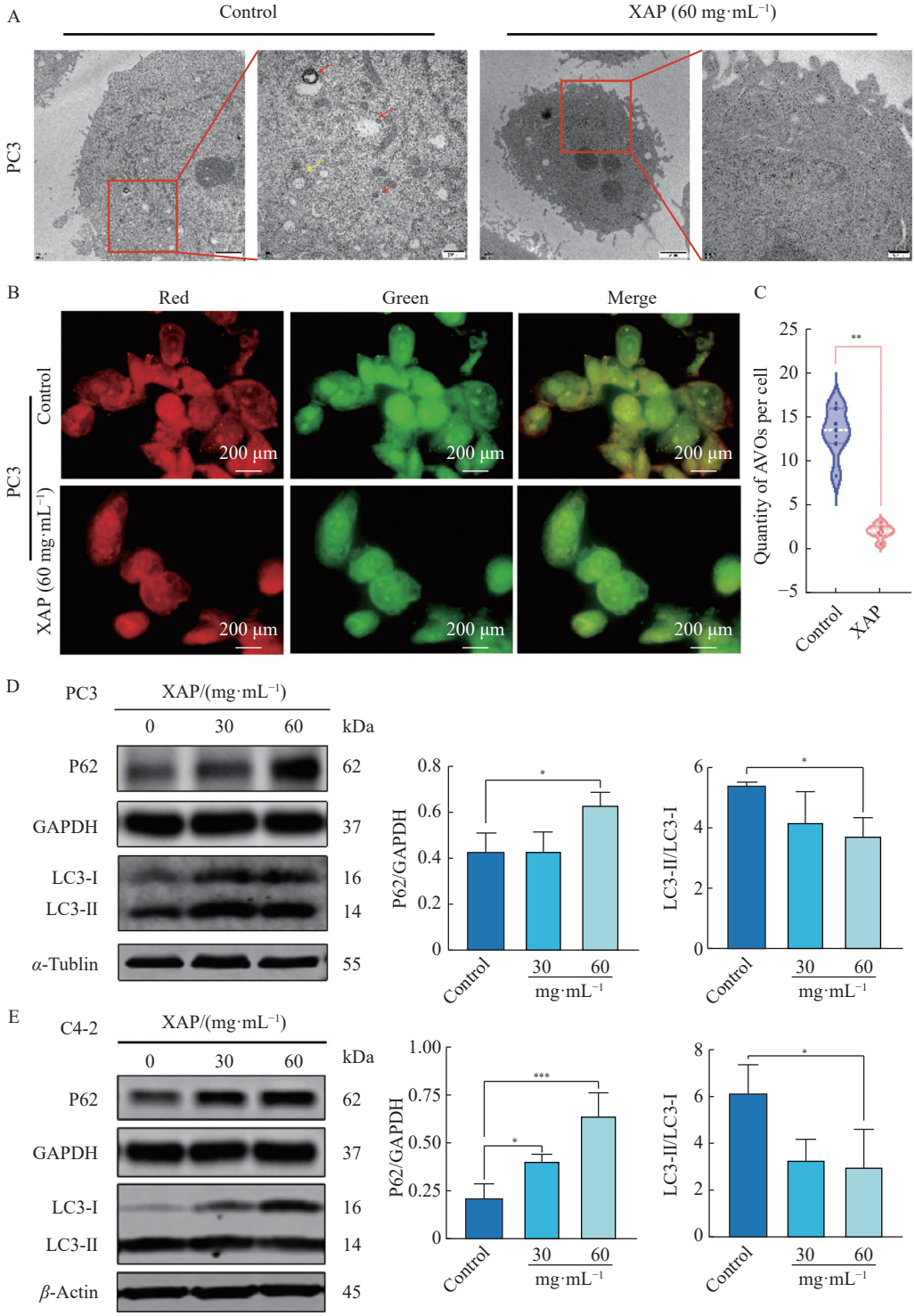

Fig. 3 XAP suppresses autophagy in PCa cells. (A) Electron microscopy images of PC3 cells exposed to XAP (0 and 60 mg·mL^{-1}) for 24 h. The control group exhibited more monolayer-structured lysosomes (red arrow) and vacuolar double-layer plasma membrane autophagosomes (yellow arrow) compared to the XAP treatment group (right scale bar = 500 nm; left scale bar = 2 μm). (B) AO staining quantification of acidic vacuolar compartments (red puncta) in PC3 cells treated with 60 mg·mL^{-1} XAP. (C) Quantification of red puncta in PC3 cells. (D–E) Western blotting analysis of LC3-II/LC3-I and P62 protein levels in C4-2 and PC3 cells treated with XAP (0, 30, and 60 mg·mL^{-1}) for 24 h. Data are expressed as mean ± SD (n = 3). $^{*}P < 0.05$, $^{**}P < 0.01$, and $^{***}P < 0.001$ *vs* control.

creased the number of acidic vesicles (Figs. 3B and 3C).

Furthermore, Western blotting analysis was employed to evaluate the classic autophagic markers: LC3-II, LC3-I, and P62. The adaptor protein P62 not only serves as a bridge between ubiquitinated substrates and LC3 but also functions as an autophagy reporter [48]. Both C4-2 and PC3 cells treated with XAP Injection exhibited elevated P62 protein levels (Figs. 3D and 3E), suggesting that XAP treatment impeded autophagic flux and substrate degradation. Following XAP administration, a decrease in the LC3-II/LC3-I ratio was observed (Figs. 3D and 3E), further demonstrating that XAP inhibited autophagy in PCa cells. Collectively, these findings indicate that XAP simultaneously suppresses autophagy and promotes apoptosis.

3.5. Atg5/Atg12 is downregulated by XAP in PCa cells, which also translocates FoxO3a into the nucleus

The synthesis of autophagosomes depends heavily on the Atg5/Atg12 conjugate [25]. XAP downregulated Atg5 and Atg12 protein expression levels (Figs. 4A–4D) without notable changes in other Atg proteins' expression levels, such as Atg3 and Atg7 (Fig. S2). Furthermore, the levels of *ATG5* and *ATG12* mRNA expression were markedly decreased in PC3 and C4-2 cells following XAP treatment for 48 h (Fig. 4E). These results indicate that XAP inhibits autophagosome formation by reducing both mRNA and protein expression levels of ATG5 and ATG12.

The FOXO signaling pathway, which regulates apoptosis and autophagy, was found to be strongly associated with XAP-induced PCa suppression, according to KEGG pathway enrichment analysis [43, 45]. This study investigated whether XAP-induced cellular apoptosis and autophagy suppression were mediated through the FOXO pathway. The results demonstrated that XAP significantly increased FoxO3a expression in C4-2 and PC3 cells (Figs. 4A–4D) without affecting FoxO1 expression (Fig. S3). To further validate the impact of XAP on elevated FoxO3a protein, the mRNA levels of *FOXO3A* were examined. The findings revealed no significant change in the mRNA expression levels of *FOXO3A* in PC3 and C4-2 cells after XAP treatment for 24 and 48 h (Fig. S4A). Therefore, the increased FoxO3a protein may result from reduced autophagy degradation rather than enhanced gene expression. In addition to inhibiting autophagy, FoxO3a translocates to the nucleus as an autophagy substrate and enhances apoptosis sensitization [44]. Following XAP administration, FoxO3a accumulated significantly and dose-dependently in the nucleus compared to the control group (Figs. 4E–4H).

To further validate the impact of XAP on FoxO3a transcription activity, we examined the mRNA levels of *PUMA*, *BIM*, and *NOXA*, downstream genes transcribed by FoxO3a, which have been identified as critical in promoting PCa cell apoptosis [49-51]. Our analysis revealed a significant increase in *NOXA* mRNA expression in C4-2 and PC3 cells (Fig. 4I) following XAP administration for 24 and 48 h, while *PUMA* and *BIM* expression levels remained unchanged after XAP treatment (Figs. S4B–S4C). These findings collectively demonstrate that XAP-induced suppression of Atg5/Atg12 conjugation promotes FoxO3a nuclear translocation, leading to *NOXA* transcription and subsequent PCa cell apoptosis.

3.6. Suppression of autophagy and accumulation of FoxO3a is required for XAP-elicited apoptosis in PCa cells

To explore the connection between XAP-induced apoptosis and autophagy inhibition, the autophagy activator Rapa was employed. For 24 or 48 h, PC3 cells were treated with 20 nmol·L^{-1} Rapa, 30 mg·mL^{-1} XAP, or a combination of Rapa and XAP for 24 or 48 h. XAP significantly reduced PC3 cell proliferation compared to the control, but Rapa partially mitigated this effect (Figs. 5A and 5B). The XAP group exhibited morphological characteristics of cell apoptosis, such as nuclear fragmentation and chromatin condensation, in contrast to the control group. However, these changes were reversed following Rapa administration (Fig. 5C). Apoptotic PC3 cell percentage rose from 3.10% ± 1.53% in the control group to 44.6% ± 7.68% in the group that received XAP treatment and then dropped to 11.72% ± 2.55% in the XAP + Rapa group (Fig. 5D). Moreover, Rapa treatment decreased the microtubule-associated protein 1 light chain 3 beta II/microtubule-associated protein 1 light chain 3 beta I (LC3II/LC3I) ratio and reversed the XAP-induced P62 accumulation (Figs. 5E and 5F). These results indicated a relationship between autophagy suppression and XAP-induced apoptosis.

Research has demonstrated the role of Rapa in stimulating the initiation and occurrence of autophagy, which results in phagocytosis and significant FoxO3a autophagy substrate consumption [52]. In the present study, Rapa administration substantially reduced the XAP-induced FoxO3a accumulation, although XAP increased FoxO3a buildup in PCa cells (Fig. 5G). In summary, XAP's suppression of autophagy promoted the accumulation of FoxO3a and apoptosis of PCa cells, while Rapa's promotion of autophagy significantly reduced FoxO3a accumulation and decreased the proportion of XAP-induced apoptosis. These findings indicate a connection between FoxO3a accumulation caused by autophagy suppression and XAP-induced apoptosis.

3.7. XAP inhibits the proliferation of PCa in vivo

The efficacy of XAP in cancer treatment was assessed *in vivo* using a PC3 xenograft tumor model (Fig. 6A). Following exposure to XAP and PTX, tumor size (Fig. 6B) and volume (Fig. 6C) were significantly reduced compared to the control sample. However, no notable differences in body weight were observed between the XAP-treated group and the control group (Fig. 6D). Additionally, XAP did not induce substantial changes in organ indices (Fig. 6E) or in the morphology of the spleen, liver, heart, lung, or kidney (Fig. 6F), demonstrating its low systemic toxicity *in vivo*.

3.8. XAP triggers apoptosis in vivo by inhibiting autophagy and promoting FoxO3a movement into the nucleus

XAP significantly enhanced tumor cell apoptosis in a TUNEL assay, confirming its anti-PCa properties *in vivo* (Fig. 7A). Treatment with XAP increased the proportion of apoptotic cancer cells from 1.46% ± 0.25% in the control group to 28.82% ± 5.86% in the group receiving moderate doses of XAP (Fig. 7B). Western blotting of apoptosis-related proteins (Fig. 7C) revealed that XAP administration elevated cleaved-caspase 9 protein expression levels, while PTX exposure upregulated both caspase 9 and cleaved-caspase 9 protein levels. All treatment groups exhibited reduced Bcl-2 protein levels, though only the low-dose XAP group showed a significant increase in Bax protein level. Atg5 protein levels decreased in all treatment groups relative to the control. The low-dose XAP and PTX groups demonstrated notably higher FoxO3a protein expression. Monitoring of the classical autophagy indicators LC3II/LC3I and P62 confirmed elevated P62 protein levels in the low-dose XAP group, while LC3II/LC3I ratios decreased in all treatment groups (Fig. 7D). Furthermore, IHC analysis showed that low-dose XAP treatment increased the proportion of nuclear FoxO3a^{+} cells in malignant tissues (Fig. 7E). These findings collectively suggest that XAP suppresses autophagy and induces apoptosis *in vivo*, exerting an anti-growth effect on PCa. FoxO3a appears to play a crucial role in elucidating the relationship between autophagy and apoptosis.

4. Discussion

PCa remains the most prevalent malignant neoplasm affect-

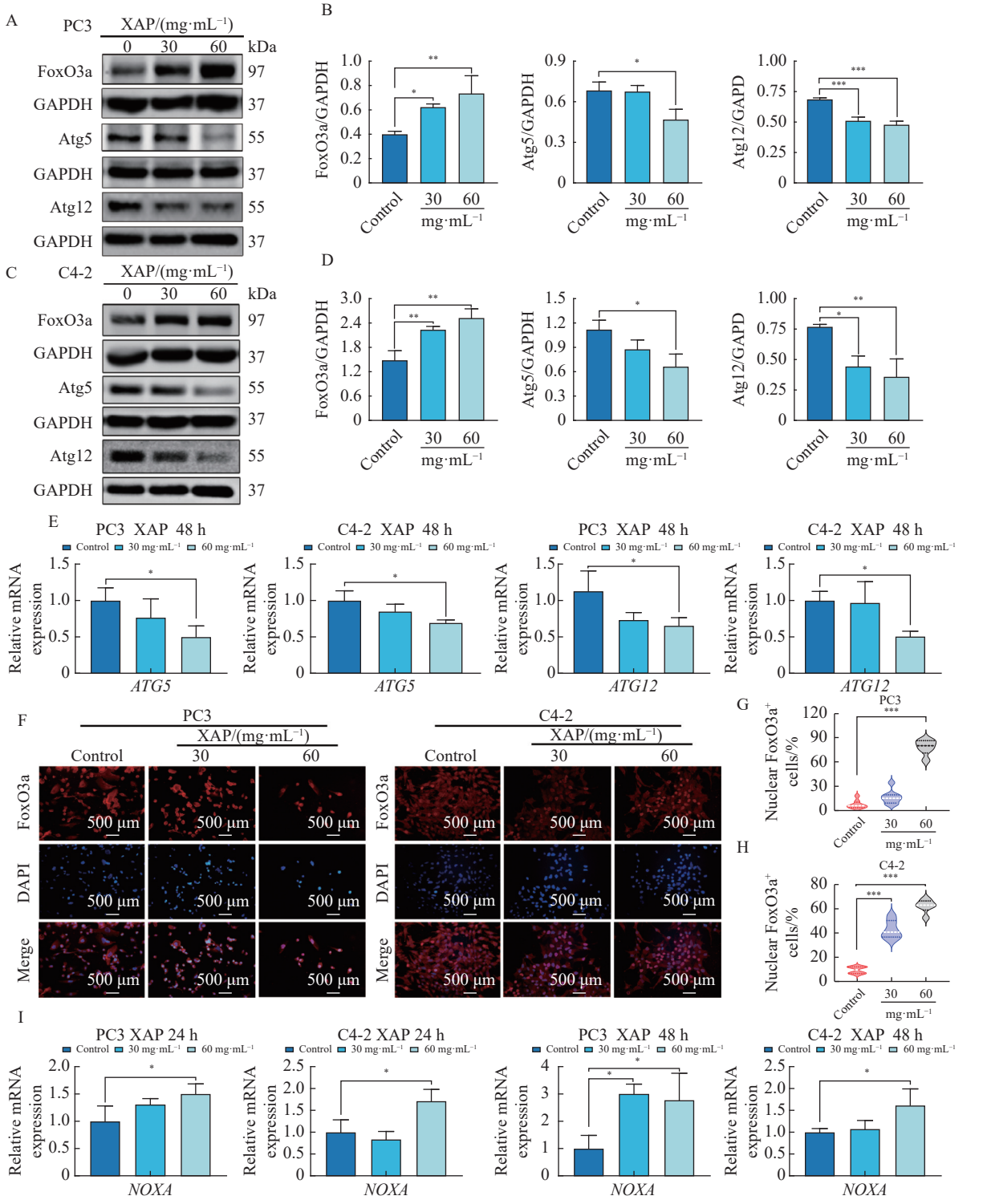

Fig. 4 XAP inhibits Atg5/Atg12 expression and enhances nuclear translocation of FoxO3a. XAP was administered to PC3 or C4-2 cells for 24 h at concentrations of 0, 30, and 60 mg·mL^{-1}. In PC3 (A, B) and C4-2 (C, D) cells, Western blotting was performed to assess the protein levels of FoxO3a, Atg5, and Atg12. (E) qRT-PCR was conducted to evaluate the *ATG5* and *ATG12* mRNA levels in C4-2 and PC3 cells. (F–H) FoxO3a expression (red) in the C4-2 (right) and PC3 (left) cells' nuclei (blue) as determined by immunofluorescence analysis. Representative images are shown (Scale bar = 500 μm). (I) qRT-PCR was performed to examine the *NOXA* mRNA levels in C4-2 and PC3 cells. Data are expressed as mean ± SD (n = 3). $^{*}P < 0.05$, $^{**}P < 0.01$, and $^{***}P < 0.001$ *vs* control.

ing older men globally [53]. In China, PCa has emerged as a significant health concern, substantially reducing both life expectancy and quality of life (QoL) due to its steadily increasing incidence [5]. Current PCa treatments, such as medroxyprogesterone acetate and bicalutamide, often result in unavoidable and adverse side effects, including intestinal damage, liver function impairment, and compromised immune response, which negatively impact patients' overall health and QoL [54]. Consequently, there is a critical need to develop novel, highly effective, and low-toxicity therapeutics for PCa. Recently, XAP has garnered considerable attention in cancer therapy due to its significant therapeutic benefits, including reduction of tumor metastasis, modulation of the TME, and counteraction of anti-tumor drug resistance [8, 16, 55]. However, the mechanisms by which XAP inhibits PCa cell proliferation remain largely elusive, significantly limiting its therapeutic applications in PCa. Our previous research, combining metabolomics and

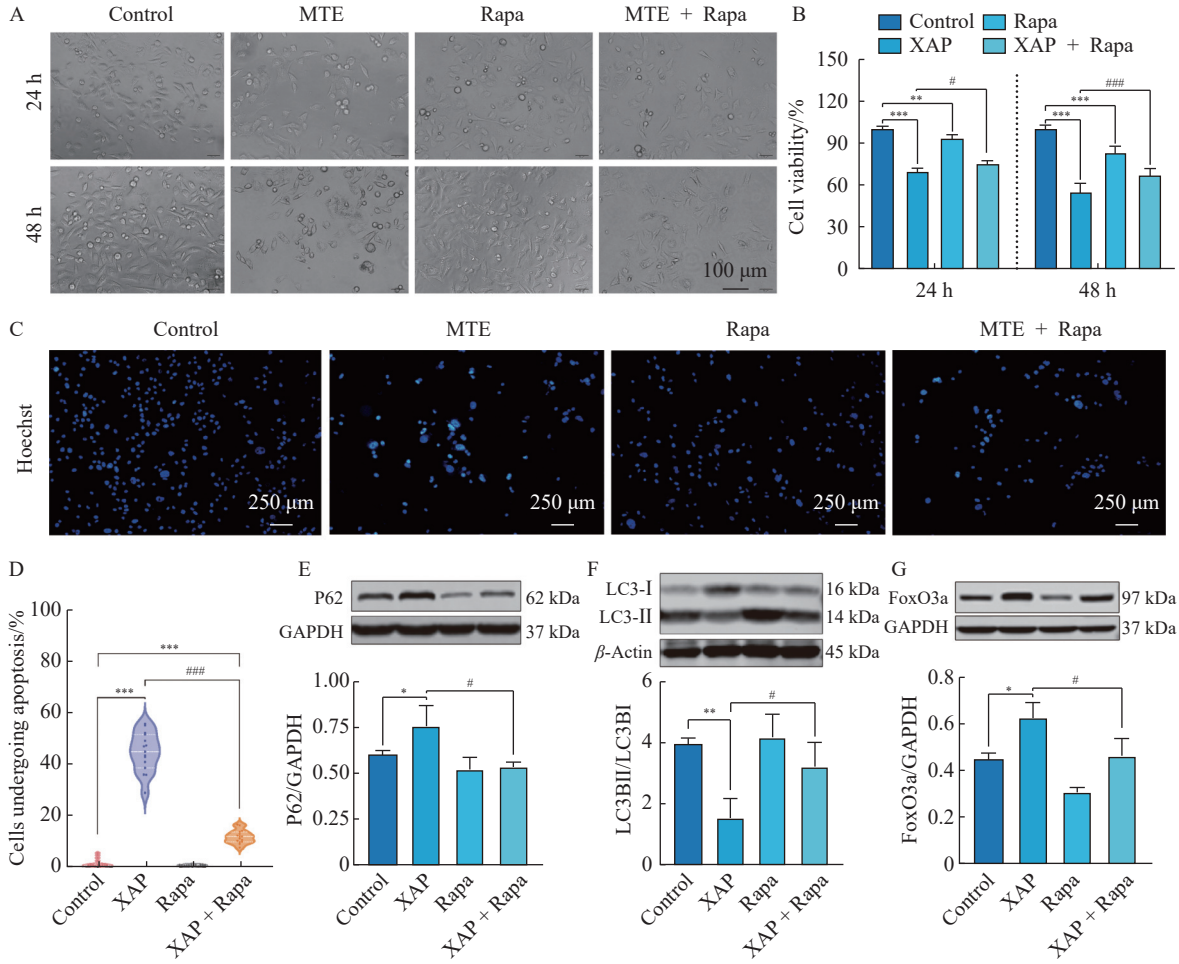

Fig. 5 Rapa counteracts apoptosis induced by XAP in PCa cells. PC3 cells were treated with 20 nmol·L^{-1} Rapa, 30 mg·mL^{-1} XAP, or Rapa + XAP for 24 or 48 h. (A, B) The morphology of PC3 cells was examined (scale bar: 100 μm), and cell viability was assessed using the CCK-8 assay. (C) After 24 h of treatment, Hoechst staining was performed to identify apoptotic PC3 cells in different groups (scale bar = 250 μm). (D) The percentage of apoptotic PC3 cells was calculated. (E–G) After 24 h of treatment, Western blotting was used to compare the protein levels of FoxO3a, LC3II/LC3I, and P62 among different groups. Data are presented as mean ± SD (n = 3). $^{*}P < 0.05$, $^{**}P < 0.01$, and $^{***}P < 0.001$ *vs* control; $^{\#}P < 0.05$ and $^{\#\#\#}P < 0.001$ *vs* XAP.

network pharmacology, revealed that XAP inhibits PCa cell proliferation *via* the human epidermal growth factor receptor 2 (ErbB2)–glycogen synthase kinase 3 (GSK3)–hypoxia-inducible factor 1 (HIF1) signaling axis [20]. The present study elucidates a novel mechanistic basis for XAP in the suppression of PCa.

Apoptosis, triggered by internal and external factors, is a pre-existing death process that eliminates damaged, mutational, or aged cells to maintain cellular homeostasis in normal tissues [56-58]. The promotion of apoptosis is a key strategy for the development of anticancer medications, as the inactivation of the apoptotic process is considered a fundamental hallmark of cancer [59]. Our previous research demonstrated that XAP may lower the mitochondrial membrane potential (MMP) and induce apoptosis in PCa cells [34], suggesting that XAP may activate the intrinsic apoptosis pathway. To validate this hypothesis, this study assessed the expression of proteins implicated in mitochondrial apoptosis, such as Bcl-2 and Bax. Our findings revealed that PCa cells and tissue samples treated with XAP exhibited significantly upregulated levels of Bax protein and markedly reduced levels of Bcl-2 protein, indicating a correlation between mitochondrial apoptosis and XAP-induced apoptosis.

Furthermore, this study demonstrates that XAP inhibits autophagy in PCa cells. Autophagy, a highly conserved catabolic process, initiates with the formation of double-membrane vesicles called autophagosomes, which engulf cellular organelles and proteins before their delivery to lysosomes [60, 61]. Autophagy plays a crucial role in tumor initiation and progression, enabling cancer cells to maintain homeostasis and adapt to stress [62]. Numerous studies have shown that autophagy inhibition suppresses proliferation, metastasis, and invasion in various malignancies, while autophagy promotion yields opposite effects [63-65]. In this study, comparative proteomics findings suggest that XAP's suppression of PCa may be associated with autophagy inhibition in addition to apoptosis induction. Consistent with this observation, TEM and AO staining experiments revealed that XAP treatment reduced autophagic vesicle formation. The significant decrease in the LC3II/LC3I ratio caused by XAP, along with increased P62 accumulation, further demonstrated XAP's inhibition of autophagy in PCa cells and tumor tissues. Moreover, XAP decreased protein levels of autophagosome formation markers Atg5 and Atg12, impeding autophagosome production [61]. Thus, XAP suppresses autophagy while promoting apoptosis. Previous reports indicate that XAP modulated autophagy and apoptosis to exert potent anticancer effects in stomach and lung cancers. Mechanistically, its anti-carcinoma activities were attributed to the activation of the ERK or AKT signaling pathways [66, 67]. However, the fundamental relationship between XAP-induced autophagy suppression and apoptosis stimulation in PCa remains uncertain.

This study revealed that FoxO3a plays a crucial role in the inhibition of autophagy and the induction of apoptosis by XAP in PCa. The FOXO pathway, particularly FoxO1 [68, 69] and FoxO3a [70, 71], regulates both apoptosis and autophagy. KEGG pathway enrichment analysis of 59 identified proteins in the current study indicated that FOXO could be a key signaling pathway in XAP-induced PCa suppression. XAP significantly enhanced FoxO3a expression

both *in vitro* and *in vivo* without altering FoxO1 levels, suggesting a critical role for FoxO3a in XAP's anti-tumor activity against PCa. When FoxO3a, a non-degradable autophagy substrate, is inhibited in PCa cells, it accumulates and subsequently translocates to the nucleus to activate pro-apoptotic proteins and initiate the apoptosis cascade [44, 72, 73]. This study demonstrates that XAP stimulated FoxO3a nuclear translocation and increased its overall cellular expression both *in vitro* and *in vivo*. Furthermore, XAP significantly elevated the mRNA level of *NOXA*, a FoxO3a downstream gene, consequently promoting apoptosis in PCa cells. These findings, combined with XAP's ability to induce apoptosis and inhibit autophagy, confirmed that FoxO3a nuclear translocation and accumulation due to autophagy suppression could be the mechanism *via* which XAP sensitizes cells to apoptosis. To further support the relationship between FoxO3a autophagic degradation and apoptosis in XAP-treated PCa cells, the autophagy agonist Rapa was employed. The results showed that Rapa inhibited XAP-induced FoxO3a accumulation and apoptosis. These findings suggest that autophagy suppression and FoxO3a accumulation in PCa cells are essential for XAP-induced apoptosis.

Our recent studies employed molecular docking to predict the active components of XAP against PCa. The analysis identified several potential active components: tenacissoside B, tenacissimoside E, marstenacisside A4, marsdenoside H, tenacissoside D, cryptochlorogenic acid, scopoletin, marsdenoside D and 12*β*-*O*-acetyl-3-*O*-(6-deoxy-3-*O*-methyl-*β*-dallopyran-osyl-(1→4)-D-oleandronyl)-11*α*-*O*-isobutyryltenacigenin B [20, 34]. Tenacissoside B, a long-acting and primary bioactive constituent in XAP Injection, has been used in treating leukocythemia, malignant tumors, and asthma [74]. While there is limited research on the pharmacological effects of tenacissimoside E, marstenacisside A4, marsdenoside H, and tenacissoside D, other identified components have been studied more extensively. Chlorogenic acid, an important phenolic compound found in various plants, including Honeysuckle, Pyrrosiae Folium, and Lonicerae Japonicae Caulis , plays a role in regulating oxidative stress and autophagy [75]. Scopoletin, a coumarin compound, has demonstrated inhibitory effects on the proliferation of cancer cells, including PCa, by controlling cell cycle and apoptosis [76]. However, further experimental validation is necessary to elucidate the precise mechanisms of

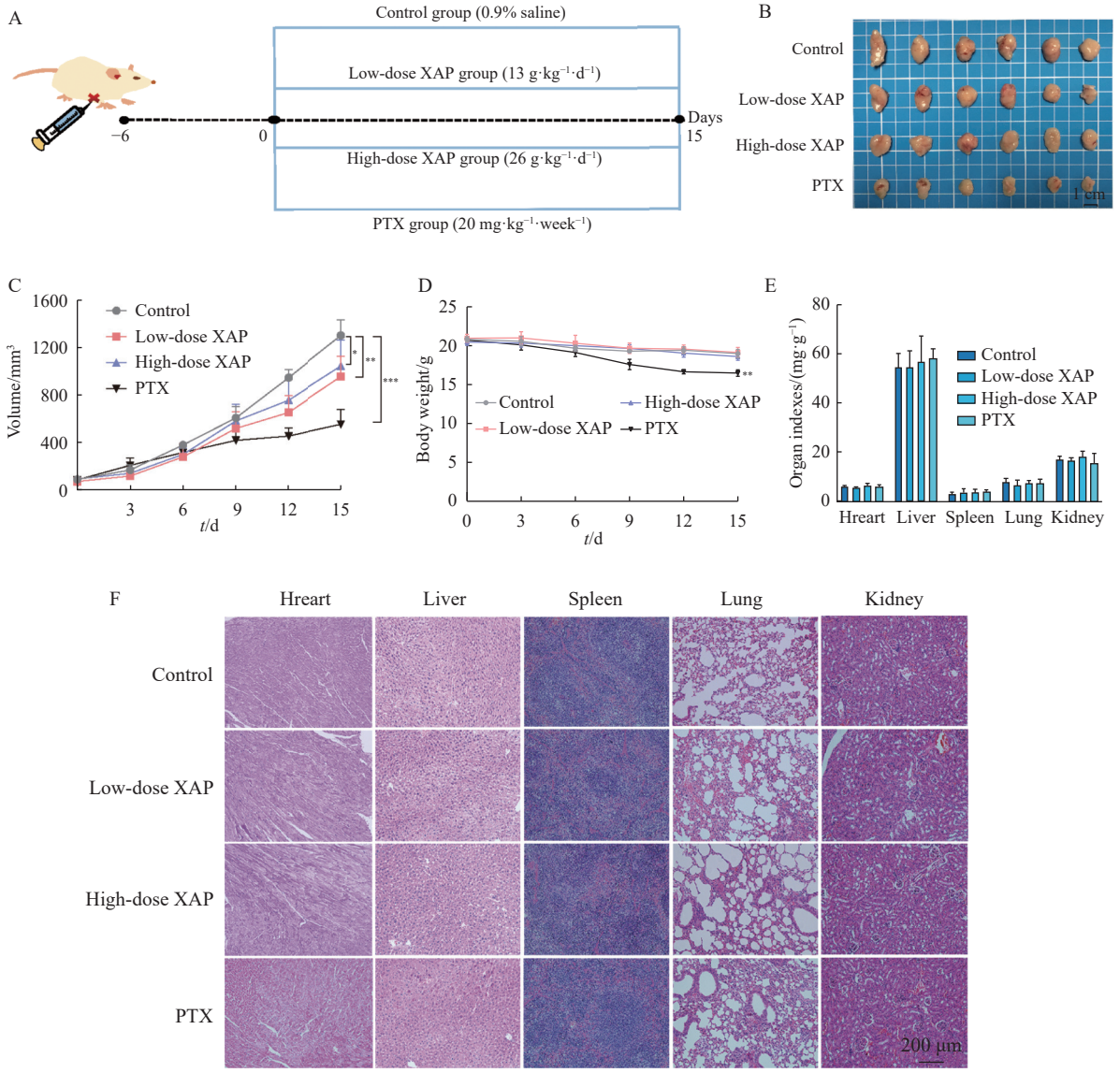

Fig. 6 *In vivo* PC3 xenograft tumor development is suppressed by XAP. (A) A concise overview of the experimental animal model. (B) Images depicting PC3 xenograft tumors in various groups at the experiment's conclusion (scale bar = 1 cm). (C) Tumor growth rates in mice across different groups throughout the treatment period. (D) Body weight trends of mice in various groups during the course of treatment. (E) Organ indices of mice in different groups at the experiment's conclusion. (F) HE staining was performed to assess the structure and morphology of organs at the end of the experiment (scale bar = 200 μm). Data are expressed as mean ± SD (n = 6). $^{*}P < 0.05$, $^{**}P < 0.01$, $^{***}P < 0.001$ *vs* control.

these components against PCa cells.

5. Conclusion

In conclusion, XAP inhibits autophagy by reducing Atg5/Atg12 levels, leading to FoxO3a accumulation and nuclear translocation. This process subsequently induces NOXA expression and promotes apoptosis in PCa cells (Fig. 8). These findings provide novel insights into the potential of XAP as a therapeutic approach for PCa treatment.

Funding

This research was supported by Guangxi Natural Science Foundation (No. 2023GXNSFDA026047), Guangxi Science and Technology Project (No. FANGKE ZY20221502), the National Natural Science Foundation of China (No. 82160948), and the Advanced Innovation Teams and Xinghu Scholars Program of

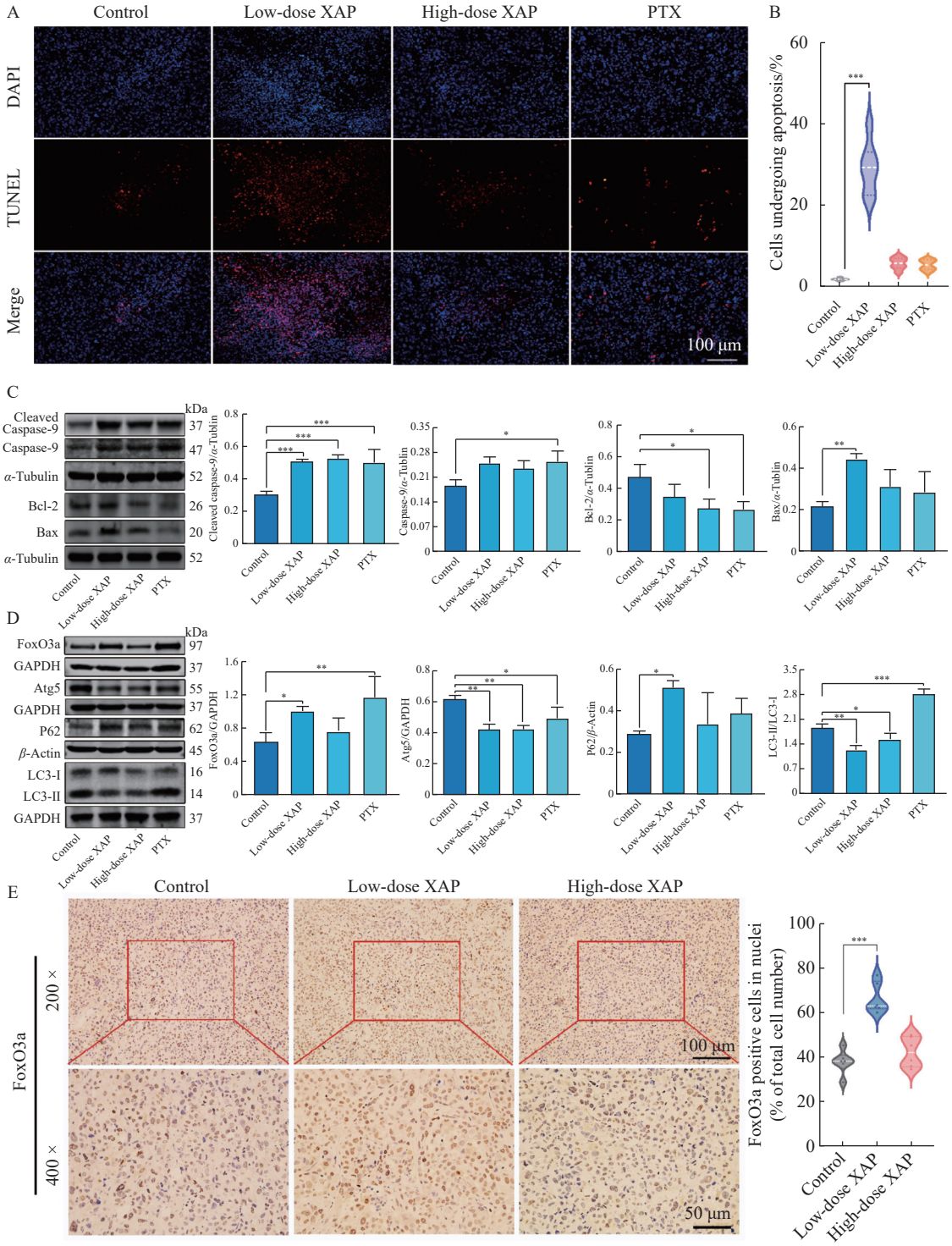

Fig. 7 XAP induces apoptosis *in vivo* by suppressing autophagy and enhancing FoxO3a nuclear translocation. (A, B) Apoptosis in tumor cells was quantified and evaluated using TUNEL labeling according to the protocol described in section 2. Representative images are shown (scale bar = 100 μm). (C, D) Levels of apoptotic and autophagy-related proteins in cancerous tissues were analyzed by Western blotting. (E) The percentage of nuclear FoxO3a$^+$ cells in malignant tissues was determined using immunohistochemical labeling (scale bar = 50 μm, below; scale bar = 100 μm, above). Data are presented as mean ± SD (n = 3). $^*P < 0.05$, $^{**}P < 0.01$, and $^{***}P < 0.001$ *vs* control.

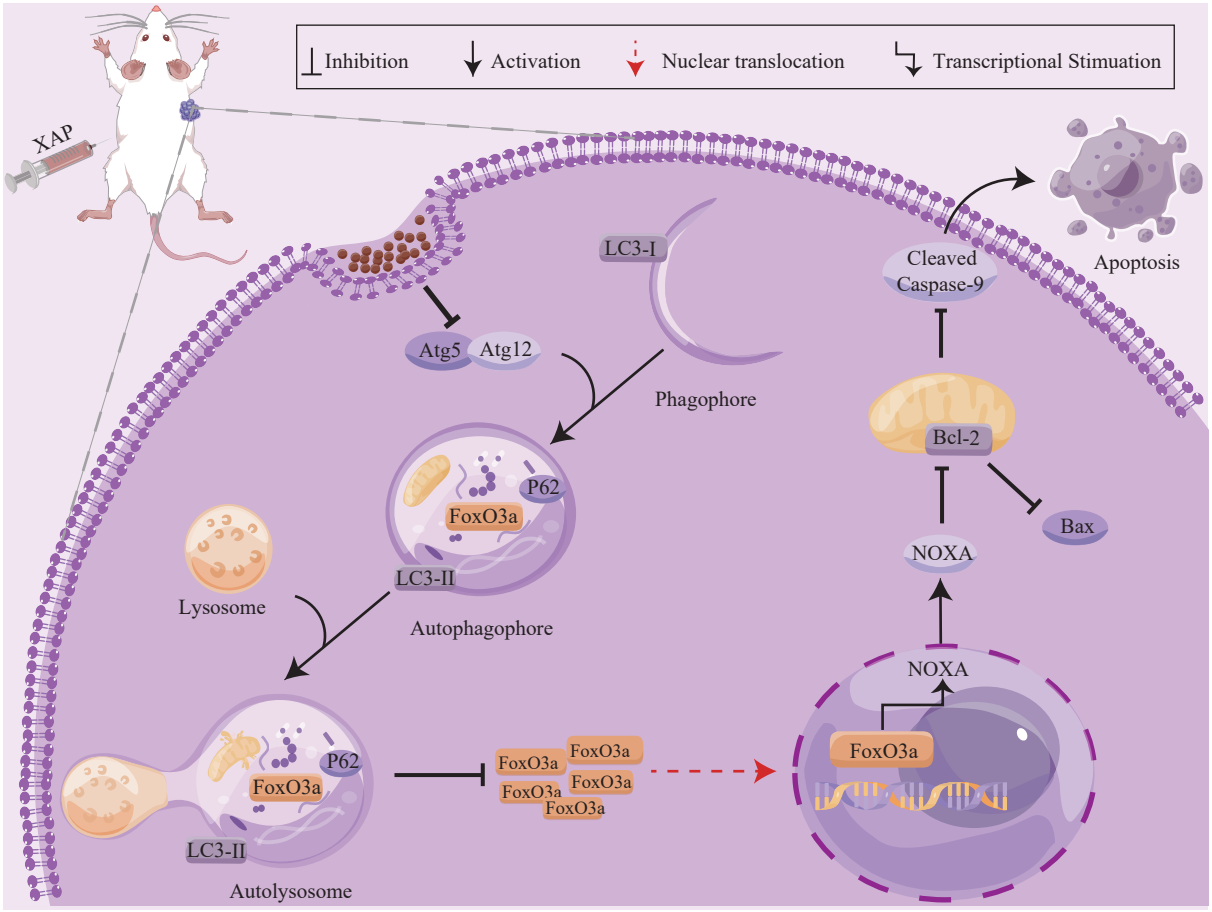

Fig. 8 Diagrammatic representation of the mechanisms underlying the inhibitory effect of XAP on PCa. XAP decreases Atg5/Atg12 expression levels, suppressing autophagy. This leads to the accumulation and nuclear translocation of the FoxO3a autophagy substrate, which activates NOXA transcription and subsequently triggers apoptosis in PCa cells.

Guangxi Medical University.

Declaration of competing interest

These authors have no conflict of interest to declare.

Supporting information

Supporting information for this study can be obtained by contacting the corresponding authors *via* E-mails.

References

1 Hyuna S, Jacques F, Rebecca LS, et al. Global cancer statistics 2020: GLOBOCAN estimates of incidence and mortality worldwide for 36 cancers in 185 countries. *CA Cancer J Clin*. 2021;71(3):209–249. https://doi.org/10.3322/caac.21660.

2 Zhai Z, Zheng Y, Li N, et al. Incidence and disease burden of prostate cancer from 1990 to 2017: results from the global burden of disease study 2017. *Cancer*. 2020;126(9):1969–1978. https://doi.org/10.1002/cncr.32733.

3 Li L, Wang J, Feng L, et al. Rubioncolin C, a natural naphthohydroquinone dimer isolated from *Rubia yunnanensis*, inhibits the proliferation and metastasis by inducing ROS-mediated apoptotic and autophagic cell death in triple-negative breast cancer cells. *J Ethnopharmacol*. 2021;277:114184. https://doi.org/10.1016/j.jep.2021.114184.

4 Tang H, Shu P, Liu S, et al. Traditional Chinese medicine in oncotherapy: the research status. *Nutr Cancer*. 2020;72(6):992–998. https://doi.org/10.1080/01635581.2019.1664599.

5 Wang X, Fang G, Pang Y. Chinese medicines in the treatment of prostate cancer: from formulas to extracts and compounds. *Nutrients*. 2018;10(3):283–298. https://doi.org/10.3390/nu10030283.

6 Zimmermann F, Papachristofilou A. Radical prostatectomy or watchful waiting in early prostate cancer. *Strahlenther Onkol*. 2019;195(11):1036–1038. https://doi.org/10.1007/s00066-019-01508-8.

7 Tian YQ, Ding P, Yan XH, et al. Discussion on quality control of preparations with cortex moutan in volume I pharmacopoeia of People's Republic of China (2005 edition). *Chin J Chin Mater Med*. 2008;33(3):339–341.

8 Zhang H, Zhang J, Ding H, et al. Clinical value of Tongguanteng (Radix Seu Herba Marsdeniae Tenacissimae) extract combined with chemotherapy in the treatment of advanced non-small cell lung cancer: a meta-analysis. *J Tradit Chin Med*. 2016;36(3):261–270. https://doi.org/10.1016/S0254-6272(16)30037-1.

9 Huang Z, Wang Y, Chen J, et al. Effect of Xiaoaiping Injection on advanced hepatocellular carcinoma in patients. *J Tradit Chin Med*. 2013;33(1):34–38. https://doi.org/10.1016/S0254-6272(13)60097-7.

10 Wang F, Fan QX, Wang HH, et al. Efficacy and safety of Xiaoaiping combined with chemotherapy in the treatment of advanced esophageal cancer. *Chin J Oncol*. 2017;39(6):453–457. https://doi.org/10.3760/cma.j.issn.0253-3766.2017.06.010.

11 Zhou X, Liu M, Ren Q, et al. Oral and injectable *Marsdenia tenacissima* extract (MTE) as adjuvant therapy to chemotherapy for gastric cancer: a systematic review. *BMC Complement Altern Med*. 2019;19(1):366–379. https://doi.org/10.1186/s12906-019-2779-y.

12 Yi B, Zhang S, Yan S, et al. *Marsdenia tenacissima* enhances immune response of tumor infiltrating T lymphocytes to colorectal cancer. *Front Immunol*. 2023;14:1238694. https://doi.org/10.3389/fimmu.2023.1238694.

13 Zhao C, Hao H, Zhao H, et al. *Marsdenia tenacissima* extract promotes gefitinib accumulation in tumor tissues of lung cancer xenograft mice *via* inhibiting ABCG2 activity. *J Ethnopharmacol*. 2020;255:112770. https://doi.org/10.1016/j.jep.2020.112770.

14 Yuan Y, Guo Y, Guo ZW, et al. *Marsdenia tenacissima* extract induces endoplasmic reticulum stress-associated immunogenic cell death in non-small cell lung cancer cells through targeting AXL. *J Ethnopharmacol*. 2023;314:116620. https://doi.org/10.1016/j.jep. 2023.116620.

15 Zhang XQ, Ding YW, Chen JJ, et al. Xiaoaiping Injection enhances paclitaxel efficacy in ovarian cancer *via* pregnane X receptor and its downstream molecules. *J Ethnopharmacol*. 2020;5(39):113067. https://doi.org/10.1016/j.jep.2020.113067.

16 Li Z, Hao H, Tian W, et al. Nitric oxide, a communicator between tumor cells and endothelial cells, mediates the anti-tumor effects of *Marsdenia tenacissima* extract (MTE). *J Ethnopharmacol*. 2020;250:112524. https://doi.org/10.1016/j.jep.2019.112524.

17 Fan W, Sun L, Zhou JQ, et al. *Marsdenia tenacissima* extract induces G_0/G_1 cell cycle arrest in human esophageal carcinoma cells by inhibiting mitogen-activated protein kinase (MAPK) signaling pathway. *Chin J Nat Med*. 2015;13(6):428–437. https://doi.org/10.1016/S1875-5364(15)30036-4.

18 Huang Z, Lin H, Wang Y, et al. Studies on the anti-angiogenic effect of *Marsdenia tenacissima* extract *in vitro* and *in vivo*. *Oncol Lett*. 2013;5(3):917–922. https://doi.org/10.3892/ol.2013.1105.

19 Wang X, Tian N, Zhng S, et al. Clinical study on rectal administration of Xiao'aiping Injection combined with chemotherapy in the treatment of prostate cancer. *Chin Pharm*. 2019;28(16):48–50. https://doi.org/10.3969/j.issn.1006- 4931. 2019.16.015.

20 Chen X, Luo Z, Liu X, et al. *Marsdenia tenacissima* (Roxb.) Moon injection

exerts a potential anti-tumor effect in prostate cancer through inhibiting ErbB2-GSK3β-HIF1α signaling axis. *J Ethnopharmacol*. 2022;295: 115381. https://doi.org/10.1016/j.jep.2022.115381.
21 Anderson MJ, Viars CS, Czekay S, et al. Cloning and characterization of three human forkhead genes that comprise an FKHR-like gene subfamily. *Genomics*. 1998;47(2):187–199. https://doi.org/10.1006/geno.1997.5122.
22 Liu Z, Li Y, She G, et al. Resveratrol induces cervical cancer HeLa cell apoptosis through the activation and nuclear translocation promotion of FOXO3a. *Pharmazie*. 2020;75(6):250–254. https://doi.org/10.1691/ph.2020.0386.
23 Liang C, Dong Z, Cai X, et al. Hypoxia induces sorafenib resistance mediated by autophagy *via* activating FOXO3a in hepatocellular carcinoma. *Cell Death Dis*. 2020;11(11):1017–1029. https://doi.org/10.1038/s41419-020-03233-y.
24 Cao Y, Li P, Wang H, et al. SIRT3 promotion reduces resistance to cisplatin in lung cancer by modulating the FOXO3/CDT1 axis. *Cancer Med*. 2021;10(4): 1394–1404. https://doi.org/10.1002/cam4.3728.
25 Noboru M. Autophagy: process and function. *Genes Dev*. 2007;21(22): 2861–2873. https://doi.org/10.1101/gad.1599207.
26 Guo Y, Zhao Y, Zhou Y, et al. LZ-101, a novel derivative of danofloxacin, induces mitochondrial apoptosis by stabilizing FOXO3a *via* blocking autophagy flux in NSCLC cells. *Cell Death Dis*. 2019;10(7):484–497. https://doi.org/10.1038/s41419-019-1714-y.
27 Lan T, Li Q, Chang M, et al. Lei-Gong-Gen Formula Granule attenuates hyperlipidemia in rats *via* cGMP-PKG signaling pathway. *J Ethnopharmacol*. 2020;260:112989. https://doi.org/10.1016/j.jep.2020.112989.
28 Li Q, Lan T, He S, et al. A network pharmacology-based approach to explore the active ingredients and molecular mechanism of Lei-Gong-Gen Formula Granule on a spontaneously hypertensive rat model. *Chin Med*. 2021;16(1): 99–119. https://doi.org/10.1186/s13020-021-00507-1.
29 Chang M, Zhu D, Chen Y, et al. Total flavonoids of litchi seed attenuate prostate cancer progression *via* inhibiting AKT/mTOR and NF-κB signaling pathways. *Front Pharmacol*. 2021;12:758219. https://doi.org/10.3389/fphar.2021.758219.
30 Zhang W, Chen T, Yang P, et al. Total flavonoids of *Litchi chinensis* Sonn. seed inhibit prostate cancer growth in bone by regulating the bone microenvironment *via* inactivation of the HGFR/NF-κB signaling pathway. *J Ethnopharmacol*. 2024;319(Pt 3):117327. https://doi.org/10.1016/j.jep.2023.117327.
31 KOUMTEBAYE E, SU N, HU W, et al. Antitumor activity of Xiaoaiping Injection on human gastric cancer SGC-7901 cells. *Chin J Nat Med*. 2012; 10(5):339–346. https://doi.org/10.1016/S1875-5364(12)60068-5.
32 Li L, Zhang W, Devanatha DSV, et al. Synthesis and characterization of gold nanoparticles from *Marsdenia tenacissima* and its anticancer activity of liver cancer HepG2 cells. *Artif Cells Nanomed Biotechnol*. 2019;47(1):3029–3036. https://doi.org/10.1080/21691401.2019.1642902.
33 Wang K, Liu W, Xu Q, et al. Tenacissoside G synergistically potentiates inhibitory effects of 5-fluorouracil to human colorectal cancer. *Phytomedicine*. 2021;86:153553. https://doi.org/10.1016/j.phymed.2021.153553.
34 Li XL, He SH, Liang W, et al. *Marsdenia tenacissima* (Roxb.) Moon Injection induces apoptosis of prostate cancer by regulating AKT/GSK3β/STAT3 signaling axis. *Chin J Nat Med*. 2023;21(2):113–126. https://doi.org/10.1016/S1875-5364(23)60389-9.
35 Julia R, Marta W, Iosune I, et al. Mechanism and functions of membrane binding by the Atg5-Atg12/Atg16 complex during autophagosome formation. *EMBO J*. 2012;31(22):4304–4317. https://doi.org/10.1038/emboj.2012.278.
36 Pu WJ, Chu XH, Guo HL, et al. The activated ATM/AMPK/mTOR axis promotes autophagy in response to oxidative stress-mediated DNA damage co-induced by molybdenum and cadmium in duck testes. *Environ Pollut*. 2023;316(P2):120574. https://doi.org/10.1016/j.envpol.2022.120574.
37 Chen B, Lai J, Dai D, et al. PARPBP is a prognostic marker and confers anthracycline resistance to breast cancer. *Ther Adv Med Oncol*. 2020;12: 1758835920974212. https://doi.org/10.1177/1758835920974212.
38 Bhanu P, Srimadhavi R, Sivapriya K. Targeting ATM and ATR for cancer therapeutics: inhibitors in clinic. *Drug Discov Today*. 2023;28(8):103662. https://doi.org/10.1016/j.drudis.2023.103662.
39 Wang XM, Lu Y, Song YM, et al. Integrative genomic study of Chinese clear cell renal cell carcinoma reveals features associated with thrombus. *Nat Commun*. 2020;11(1):739. https://doi.org/10.1038/s41467-020-14601-9.
40 Jiang L, Zhao YM, Yang MZ. Inhibition of autophagy enhances apoptosis induced by bortezomib in AML cells. *Oncol Lett*. 2021;21(2):109–115. https://doi.org/10.3892/ol.2020.12370.
41 Angelica G, Ilenia C, Francesco P, et al. The mitomiR/Bcl-2 axis affects mitochondrial function and autophagic vacuole formation in senescent endothelial cells. *Aging*. 2018;10(10):2855–2873. https://doi.org/10.18632/aging.101591.
42 Zhou Y, Lu X, Huang D, et al. A novel protease inhibitor causes inclusion vacuole reduction and disrupts the intracellular growth of chlamydia trachomatis. *Biochem Biophys Res Commun*. 2019;516(1):157–162. https://doi.org/10.1016/j.bbrc.2019.05.184.
43 Manuel D, Michel H, Jörg W, et al. Wnt signaling inhibits Forkhead box O3a-induced transcription and apoptosis through up-regulation of serum- and glucocorticoid-inducible kinase 1. *J Biol Chem*. 2008;283(28):19201–19210. https://doi.org/10.1074/jbc.M710366200.
44 Jiang K, Zhang C, Yu B, et al. Autophagic degradation of FOXO3a represses the expression of PUMA to block cell apoptosis in cisplatin-resistant osteosarcoma cells. *Am J Cancer Res*. 2017;7(7):1407–1422.
45 Fitzwalter BE, Andrew T. FOXO3 links autophagy to apoptosis. *Autophagy*. 2018;14(8):1467–1468. https://doi.org/10.1080/15548627.2018.1475819.
46 Klionsky DJ. Autophagy revisited: a conversation with Christian de Duve. *Autophagy*. 2008;4(6):740–743. https://doi.org/10.4161/auto.6398.
47 Gjedde PM. Acridine orange as a probe for measuring pH gradients across membranes: mechanism and limitations. *Anal Biochem*. 1991;192(2):316–321. https://doi.org/10.1016/0003-2697(91)90542-2.
48 Moscat J, Karin M, Diaz-Meco MT. p62 in cancer: signaling adaptor beyond autophagy. *Cell*. 2016;167(3):606–609. https://doi.org/10.1016/j.cell.2016.09.030.
49 Sun J, Cao Q, Lin S, et al. Knockdown of CALM2 increases the sensitivity to afatinib in HER2-amplified gastric cancer cells by regulating the Akt/FoxO3a /Puma axis. *Toxicol In Vitro*. 2023;87:105531. https://doi.org/10.1016/j.tiv.2022.105531.
50 Seiji A, Andreas V, Mannan N, et al. MARCH5 mediates NOXA-dependent MCL1 degradation driven by kinase inhibitors and integrated stress response activation. *eLife*. 2020;9:54954. https://doi.org/10.7554/eLife.54954.
51 Zheng C, Yu X, Liang Y, et al. Targeting PFKL with penfluridol inhibits glycolysis and suppresses esophageal cancer tumorigenesis in an AMPK/FOXO3a/BIM-dependent manner. *Acta Pharm Sin B*. 2022;12(3):1271–1287. https://doi.org/10.1016/j.apsb.2021.09.007.
52 Zhang X, Zhang W, Wang Z, et al. Enhanced glycolysis in granulosa cells promotes the activation of primordial follicles through mTOR signaling. *Cell Death Dis*. 2022;13(1):87. https://doi.org/10.1038/s41419-022-04541-1.
53 Siegel RL, Miller KD, Fuchs HE, et al. Cancer statistics, 2021. *CA Cancer J Clin*. 2021;71(1):7–33. https://doi.org/10.3322/caac.21654.
54 Cao LY, Huang H, Ni JH. Progress in researches on drugs for prostate cancer. *Natl J Androl*. 2003;9(9):703–706.
55 Jiang S, Qiu L, Li Y, et al. Effects of *Marsdenia tenacissima* polysaccharide on the immune regulation and tumor growth in H22 tumor-bearing mice. *Carbohydr Polym*. 2016;137:52–58. https://doi.org/10.1016/j.carbpol.2015.10.056.
56 Baig S, Seevasant I, Mohamad J, et al. Potential of apoptotic pathway-targeted cancer therapeutic research: where do we stand. *Cell Death Dis*. 2016;7:2058–2068. https://doi.org/10.1038/cddis.2015.275.
57 Jan R, Chaudhry GE. Understanding apoptosis and apoptotic pathways targeted cancer therapeutics. *Adv Pharm Bull*. 2019;9(2):205–218. https://doi.org/10.15171/apb.2019.024.
58 Renehan AG, Booth C, Potten CS. What is apoptosis, and why is it important. *BMJ*. 2001;322(7301):1536–1538. https://doi.org/10.1136/bmj.322.7301.1536.
59 Hanahan D, Weinberg RA. The hallmarks of cancer. *Cell*. 2000;100(1): 57–70. https://doi.org/10.1016/S0092-8674(00)81683-9.
60 Li W, Luo LX, Zhou QQ, et al. Phospholipid peroxidation inhibits autophagy *via* stimulating the delipidation of oxidized LC3-PE. *Redox Biol*. 2022;55: 102421. https://doi.org/10.1016/j.redox.2022.102421.
61 Mizushima N, Yoshimori T, Ohsumi Y. The role of Atg proteins in autophagosome formation. *Annu Rev Cell Dev Biol*. 2011;27:107–132. https://doi.org/10.1146/annurev-cellbio-092910-154005.
62 Galluzzi L, Pietrocola F, Bravo-San PJM, et al. Autophagy in malignant transformation and cancer progression. *EMBO J*. 2015;34(7):856–880. https://doi.org/10.15252/embj.201490784.
63 Dong J, Zhu C, Zhang F, et al. "Attractive/adhesion force" dual-regulatory nanogels capable of CXCR4 antagonism and autophagy inhibition for the treatment of metastatic breast cancer. *J Control Release*. 2022;341:892–903. https://doi.org/10.1016/j.jconrel.2021.12.026.
64 Wang Z, Yang L, Wu P, et al. The circROBO1/KLF5/FUS feedback loop regulates the liver metastasis of breast cancer by inhibiting the selective autophagy of afadin. *Mol Cancer*. 2022;21(1):29–47. https://doi.org/10.1186/s12943-022-01498-9.
65 Li M, Zhao X, Yong H, et al. FBXO22 promotes growth and metastasis and inhibits autophagy in epithelial ovarian cancers *via* the MAPK/ERK pathway. *Front Pharmacol*. 2021;12:778698. https://doi.org/10.3389/fphar.2021.778698.
66 Jiao YN, Wu LN, Xue D, et al. *Marsdenia tenacissima* extract induces apoptosis and suppresses autophagy through ERK activation in lung cancer cells. *Cancer cell Int*. 2018;18:149. https://doi.org/10.1186/s12935-018-0646-4.
67 Li K, Hao K, Zhang Y, et al. C21 fraction refined from *Marsdenia tenacissima*-induced apoptosis is enhanced by suppression of autophagy in human gastric cell lines. *ACS Omega*. 2020;5(39):25156–25163. https://doi.org/10.1021/acsomega.0c02748.
68 Han RH, Huang HM, Han H, et al. Propofol postconditioning ameliorates hypoxia/reoxygenation induced H9c2 cell apoptosis and autophagy *via* upregulating forkhead transcription factors under hyperglycemia. *Mil Med Res*. 2021;8(1):58. https://doi.org/10.1186/s40779-021-00353-0.
69 Hao H, Bai Y, Liu Y, et al. Protective mechanism of FoxO1 against early brain injury after subarachnoid hemorrhage by regulating autophagy. *Brain Behav*. 2021;11(11):2376. https://doi.org/10.1002/brb3.2376.
70 Du JF, Xu Q, Zhao H, et al. PI3K inhibitor 3-MA promotes the antiproliferative activity of esomeprazole in gastric cancer cells by downregulating EGFR *via* the PI3K/FOXO3a pathway. *Biomed Pharmacother*. 2022;148:112665. https://doi.org/10.1016/J.BIOPHA.2022.112665.
71 Nirmala TP, Naeun L, Hoon SS, et al. Pitavastatin induces cancer cell apoptosis by blocking autophagy flux. *Front Pharmacol*. 2022;13:854506. https://doi.org/10.3389/fphar.2022.854506.
72 Fitzwalter BE, Towers CG, Sullivan KD, et al. Autophagy inhibition mediates apoptosis sensitization in cancer therapy by relieving FOXO3a turnover. *Dev Cell*. 2018;44(5):555–565. https://doi.org/10.1016/j.devcel.2018.02.014.
73 Lei S, Soon L, Cheon JJ, et al. *Chelidonium majus* induces apoptosis of human ovarian cancer cells *via* ATF3-mediated regulation of Foxo3a by Tip60. *J Microbiol Biotechnol*. 2022;32(4):493–503. https://doi.org/10.4014/jmb.2109.09030.
74 Li SY, Pei WH, Zhang H. Simultaneous determination of eight bioactive components in *Marsdenia tenacissima* extract in rat plasma by LC-MS/MS and its application in a pharmacokinetic study. *Biomed Chromatogr*. 2020;34 (11):e4946. https://doi.org/10.1002/bmc.4946.
75 Ji X, Wang B, Nath PY, et al. Protective effect of chlorogenic acid and its analogues on lead-induced developmental neurotoxicity through modulating oxidative stress and autophagy. *Front Mol Biosci*. 2021;8:655549. https://doi.org/10.3389/fmolb.2021.655549.
76 Li CL, Han XC, Zhang H, et al. Effect of scopoletin on apoptosis and cell cycle arrest in human prostate cancer cells *in vitro*. *Trop J Pharm Res*. 2015;14(4): 611–617. https://doi.org/10.4314/tjpr.v14i4.8.